MR acoustic radiation force imaging: *In vivo* comparison to ultrasound motion tracking

Yuexi Huang,[a] Laura Curiel,[b] and Aleksandra Kukic[c]
Sunnybrook Health Sciences Centre, Toronto, Ontario M4N 3M5, Canada

Donald B. Plewes[d]
Sunnybrook Health Sciences Centre, Toronto, Ontario M4N 3M5, Canada and Department of Medical Biophysics, University of Toronto, Toronto, Ontario M4N 3M5, Canada

Rajiv Chopra[e]
Sunnybrook Health Sciences Centre, Toronto, Ontario M4N 3M5, Canada

Kullervo Hynynen[f]
Sunnybrook Health Sciences Centre, Toronto, Ontario M4N 3M5, Canada and Department of Medical Biophysics, University of Toronto, Toronto, Ontario M4N 3M5, Canada

(Received 12 December 2008; revised 26 March 2009; accepted for publication 26 March 2009; published 5 May 2009)

MR acoustic radiation force (ARF) imaging was developed for measuring tissue elastic properties using focused ultrasound to deliver a localized tissue motion. In this study, an imaging ultrasound transducer was mounted on the focused ultrasound transducer and ultrasound motion tracking was performed simultaneously to MR ARF imaging to validate the measurement results. *In vivo* studies on rabbit thigh muscle were performed and results showed a general agreement between the two modalities (slope=0.96 and R^2=0.67). The temporal information by the ultrasound measurement indicates that the parameters in MR ARF imaging should be optimized according to the tissue type, acoustic power, and envelope and frequency of the ARF modulation. © *2009 American Association of Physicists in Medicine*. [DOI: 10.1118/1.3120289]

Key words: acoustic radiation force, elastography, tissue displacement, local harmonic motion, focused ultrasound

I. INTRODUCTION

Changes in tissue elasticity are generally associated with pathological development, such as tumor and infarction, and are commonly observed in interventional treatments, especially after thermal ablation. Therefore, detecting the changes in tissue elasticity plays an important role in diagnosis and treatment monitoring. In the past two decades, elastography techniques have been developed in magnetic resonance imaging (MRI) and ultrasound imaging for measuring elastic properties of tissue.[1–6] Conventionally, compressional or vibrational force is applied on the tissue surface by a mechanical device, which generates longitudinal or shear waves propagating into the tissue. The local displacement of tissue is then measured by motion-encoding gradients in magnetic resonance (MR) elastography or by correlation techniques in ultrasound elastography. Elasticity modulus or Young's modulus can be calculated from the magnitude of tissue displacement under certain assumptions.[2] In the case of shear wave imaging, tissue shear modulus can be calculated by estimating the local shear wavelength from the map of tissue displacement.[7]

An alternative way of generating tissue motion is by using acoustical radiation force (ARF) from focused ultrasound (FUS).[8–16] One advantage of this approach is potentially higher displacement amplitude at deep tissues. Furthermore, the motion is localized near the focus, therefore avoiding the complicated issues of wave reflection by bones or other structures commonly associated with surface drivers. ARF can be applied in various ways: In the quasistatic approach, a long FUS pulse is applied until a static displacement is achieved for measurement;[12] in the transient approach, a relatively short FUS pulse is applied and measurement is performed during the relaxation phase of the tissue motion;[8,10] and in the dynamic approach, the FUS is modulated at a certain frequency to establish a local harmonic motion (LHM) of the tissue.[9,11,14–16] Feasibility studies of MR ARF imaging on phantom and *ex vivo* tissue samples have demonstrated a near linear relationship between the displacement magnitude and the acoustic power.[11,12] However, in calculating the displacement values, simplified models of motion under ARF were applied, assuming either sinusoidal motion under the dynamic approach[9,11] or static displacement under the quasistatic approach.[12] These assumptions depend on the elasticity of tissue and the applied radiation force and have not been validated *in vivo*. On the other hand, ultrasound ARF measurement is able to track the motion in real time and therefore can provide helpful temporal information. To our knowledge a strict *in vivo* comparison between dynamic US measures of tissue stiffness and that achieved by MR ARF imaging has not been presented. In this work, MR ARF imaging was applied *in vivo* on rabbit

thigh muscle simultaneously with ultrasound LHM measurement, by which time-resolved displacement values during the MR measurement were tracked. Time-averaged results from the two modalities were compared.

II. METHODS

II.A. Ultrasound ARF measurement

Ultrasound ARF measurement was performed in a LHM imaging approach.[14–16] A single-element spherical shell FUS transducer (100 mm diameter, 80 mm focal length) with a central frequency of 1.485 MHz was modulated by rectangular-envelope pulses at 50 Hz (10 ms on and 10 ms off) to create a LHM at the focal spot. 2 cycles were needed as preparation to establish the LHM in tissues. The full width at half maximum (FWHM) intensity at the focus was 1 mm in diameter and 4 mm in the beam direction based on a needle hydrophone measurement (0.075 mm diameter, Precision Acoustics, Dorset, UK). A circular ultrasound imaging transducer (PZT 5, 1-3 piezocomposite, Imasonic, Besançon, France) was mounted inside the central hole of the FUS transducer to track the motion induced by the FUS. The focal volumes of the two transducers were aligned by hydrophone measurements. The imaging transducer had a central frequency of 5 MHz, a diameter of 20 mm, a focal length of 47 mm, and a bandwidth of 50% (at −3 dB in power). The imaging transducer was driven by a pulser/receiver (JSR300, Ultrasonics, NY) at a pulse-repetition frequency of 3 kHz. Radio frequency (RF) data representing the received echoes from the tissue were acquired at a sampling rate of 125 MHz using a PCI digitizer card (ATS460, Alazartech, Canada) and stored on a hard drive. The received signal was filtered using a 4.5–10 MHz band-pass filter to remove signal contamination from the FUS transducer and MRI. Signal tracking was performed using a cross-correlation technique with a 2 mm window.[16] Displacement estimates were made relative to the initial position immediately before the ultrasound exposure. The transducers were mounted on a MR-compatible positioning system and connected via cables to the controlling equipments outside the MR room in the console area.

II.B. MR ARF imaging

For the MR measurement, the LHM motion was repeated for the multiple phase-encoding steps. To avoid heat accumulation during the repeated pushes, 3 cycles of pushes were applied every 3 s (1% duty cycle) for each phase-encoding step. The first 2 cycles (not measured) were used to establish the LHM, and the third cycle was measured by US and MR simultaneously for the purpose of comparison. A dynamic MR elastography approach cannot be used here since the motion was not sinusoidal, which is an assumption to inversely calculate the displacement in the dynamic approach. The motion was exponential both in the compression and the relaxation phases, with the displacement flattened out near the top and the bottom. Therefore we used a quasistatic approach to measure the difference between the average motion near the top and the average motion near the bottom. Although the tissue did not reach a quasistatic state during the measurement, the average motion measured by MR can be calculated from the corresponding US measurement; therefore a comparison between the two modalities was feasible. A two-dimensional (2D) gradient-echo sequence was modified by adding bipolar gradients for motion encoding. External triggering was used to synchronize MR and ultrasound. The 5 ms positive polar gradient started 5 ms after the FUS sonication, and the 5 ms negative polar gradient started 10 ms after the stop of the sonication [Fig. 1(a)] in order to maximize the displacement difference between the bipolar gradients. Measurement with inverted gradients was subtracted to remove background phase variations. The imaging parameters were as follows: TE of 28 ms, bipolar gradient amplitude of 2 G/cm, FOV of 12 cm, 128×128 matrix, 3 mm slice thickness, and effective TR of 3 s. The scan time for the MR acquisition was about 13 min. The b value of the bipolar gradients was around 10 $\mathrm{s/mm^2}$. The displacement sensitivity was 18.7 μm/rad. A 3×3 pixel region of interest (ROI) at the focus was averaged to calculate the displacement value. MR measured the difference of the average displacement under the bipolar gradients (D_{bp}). The corresponding value by ultrasound measurement was calculated for comparison. In ultrasound calculation, 5-degree

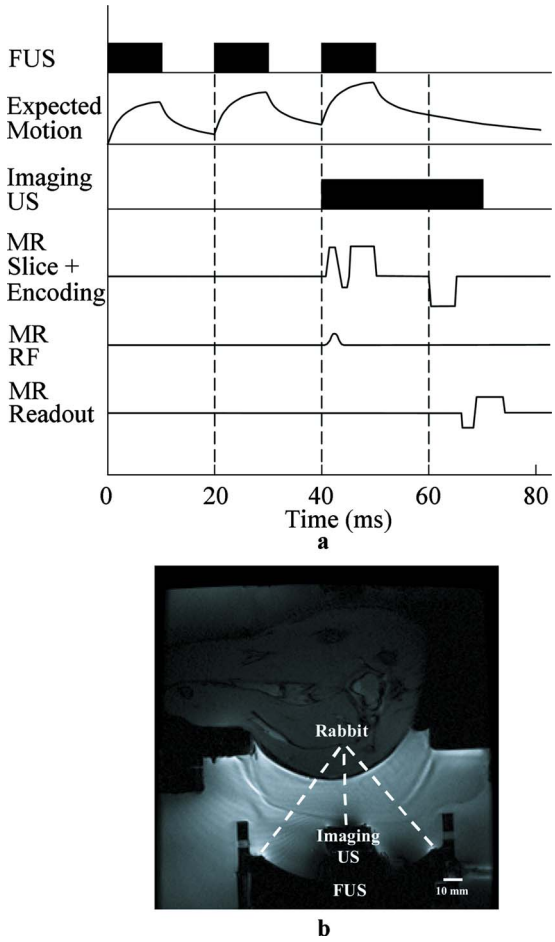

FIG. 1. (a) The timing scheme of MR and ultrasound ARF measurements and (b) *in vivo* experiment setup.

polynomial fitting was applied to remove occasional spike noise possibly due to interference from the therapeutic transducer as well as electronic noise from the equipment, which tends to affect the cross-correlation calculation of displacements.

II.C. *In vivo* experiments

In vivo experiments were performed on the thigh muscle of three rabbits on a 3 T MR scanner (GE Healthcare, Milwaukee, WI). The study protocol was approved by our institutional Animal Care Committee. The confocal ultrasound transducers were placed in a tank of degassed water to provide coupling between the transducers and the target. The acoustical window was enclosed by a thin film filled with water. A 5-inch surface coil was placed on top of the film for signal reception. A MR image of the *in vivo* experiment setup is shown in Fig. 1(b). Rabbit thighs were depilated before experiments. Measurements were performed in rabbit thigh muscles between 15 and 20 mm deep from the skin. Acoustical power of 25 W was applied and the *in situ* acoustic intensities at the focus were estimated to be between 2000 and 2300 W/cm^2 (spatial peak pulse average) depending on the depth. The acoustic intensity *in situ* was obtained from calibration measurements in water using a needle hydrophone and then taking into account the attenuation in the muscle at 4 Np/m/MHz. A manual three-dimensional (3D) positioning system enabled accurate positioning of the transducer relative to the target. MR and ultrasound ARF measurements were performed simultaneously at 14 separate locations. Because of the relatively long scan time of MR elastography and limited scan time available, only one thigh per rabbit was usable each time, i.e., 14 locations in three thighs.

III. RESULTS

The magnitude of tissue displacement varied among locations. One example of ultrasound measurement is shown in Fig. 2(a). The temporal data show that the compression and the relaxation phases of the tissue motion were near exponential when using FUS bursts of constant amplitude. Exponential fitting for the pushing phase was $d=(41.3-46.4)\times e^{(-0.31t)}$, and $d=(-4.4+277.6)\times e^{(-0.18t)}$ for the relaxation phase (t was from 0 to 10 ms and 10 to 25 ms, respectively). R^2 was 0.95 for the pushing phase and 0.93 for the relaxation phase. The time constants were found to be consistent across the measurements. Since the temporal information can only be measured by US but not by MR, the consistency of the time constants was not thoroughly investigated in this study. The calculated D_{bp} from the ultrasound data (34.7 ± 4.1 μm) was in close agreement to the MR result 30.8 ± 0.8 μm [Fig. 2(b)].

The scatter plot in Fig. 2(c) shows general agreement between the MR measurements and the calculated ultrasound data in 9 of the 14 measurements. At four other locations, the noise in the US data was so significant that off-line postprocessing could not deliver meaningful result. And at one location the MR image had susceptibility artifacts at the focal point, possibly due to cavitation effect. The slope of the linear fitting of the nine measurements was 0.96 and R^2 was 0.67. Factors that may contribute to the variability of tissue displacement seen in the figure include tissue depth and tissue surrounding structures. For tissues close to the bone, the magnitude of displacement was generally less.

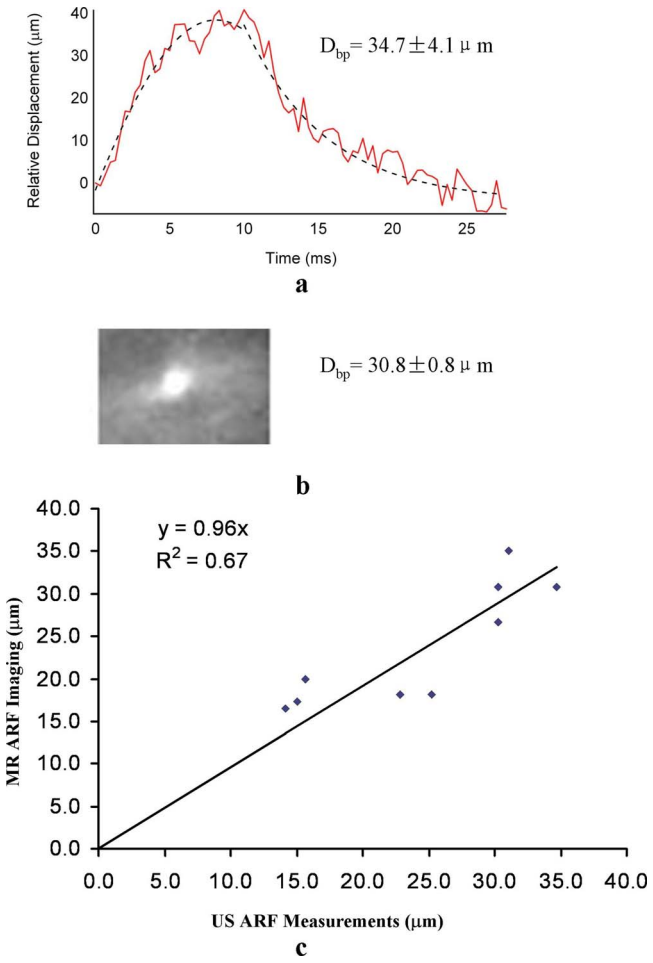

FIG. 2. Measurement results of ultrasound and MR ARF imaging. (a) One example of ultrasound measurement. The displacement values between 5 and 10 ms and 20 and 25 ms were used to calculate D_{bp} (displacement difference corresponds to the bipolar gradients in the MR measurement). The dotted line shows an exponential fitting. (b) The corresponding MR result. (c) Scatter plot of nine measurements. Measurements from the two modalities were in general agreement with a linear regression slope of 0.96 and $R^2=0.67$.

IV. DISCUSSION

In this study, a quasistatic approach was applied in MR ARF imaging. Due to the relatively high acoustic power we used, tissue motion did not reach a static state after 10 ms of FUS pushing at the modulation frequency of 50 Hz, as showed by the ultrasound measurement. Ultrasound result also showed that tissue motion under acoustic radiation force of constant amplitude was near exponential, with the relaxation phase slower than the compression phase. Therefore, it is inappropriate to assume that the result in our quasistatic MR ARF imaging shows the maximum displacement or to

use a sinusoid model to solve the displacement map in the dynamic approach. The acoustic power and modulation frequency of FUS in this study were adopted from the setup of an ultrasound LHM system which was developed for real-time monitoring of FUS thermal ablation. Therefore, both of the parameters were chosen in the context of therapeutic treatment. If the purpose of ARF imaging is for diagnostic applications, a lower acoustic power can be used with reduced displacement magnitude and reduced time for tissue to reach a static displacement. If dynamic MR ARF imaging is of interest, sinusoidal FUS modulation and its optimal frequency should be investigated for a more controlled motion profile *in vivo*.

In MR imaging, both temperature change and motion contribute to phase dispersion. In MR elastography, phase changes due to temperature have to be avoided or corrected. In our experiment setup (3 cycles of 10 ms sonications every 3 s), MR thermometry was performed to confirm that the temperature elevation over the time of the MR elastography measurement was less than the measurement noise (± 0.3 °C). However, it is difficult to directly measure the temperature rise during the sonication. We estimated its magnitude by interpolating the data of temperature measurement using the same acoustic power as used in elastography in continuous mode. The measurement showed a temperature elevation of 25.7 ± 0.3 °C over 25 s. We assumed that the temperature elevation was close to linear;[17,18] therefore the temperature change over 10 ms was estimated as approximately 0.01 °C. This magnitude of temperature change contributed to about 0.002 rad phase change in our elastography measurement and was one order of magnitude below the phase noise level (~0.03 rad). Therefore the influence of temperature-induced phase changes was considered negligible in our experiment. Applying a lower acoustic power would reduce heat accumulation and therefore can speed up the MR measurement.

The displacement measured by MR was the average value of a 3×3 pixel ROI ($2.8 \times 2.8 \times 3.0$ mm^3). The focal volume of the imaging US transducer was 1×1 mm^2 on the transverse plane and about 0.4 mm on the axial dimension. Despite the significant difference of signal volumes between the two measurements, we expect that the tissue was smoothly interconnected with their surrounding tissue; therefore the correlation of the two measurements should remain to be high.

In previous studies of MR ARF imaging, one-dimensional (1D) line scan techniques were developed for fast MR measurement after every single FUS push.[11,12] The line scan approach removes the need for repeated FUS pushes for 2D imaging and is therefore more efficient and appropriate. Furthermore, line scan techniques are less sensitive to respiratory motion for *in vivo* measurement. However, the signal-to-noise ratio (SNR) of the line scan is generally low due to a limited scan time. To improve the SNR, either temporal averaging of repeated lines is needed or the lateral dimensions of the line need to be prescribed large enough for volume averaging. In either case, the advantage of the line scan is compromised. Particularly, for the comparison of MR and ultrasound results, it is also easier to find the focal spot in the 2D MR image retrospectively than to prescribe it precisely during the measurement. Therefore, to better compare the results quantitatively, the 2D approach was used in this study.

In conclusion, the measurement result of MR ARF imaging was validated by the ultrasound measurement performed simultaneously in this study. In situations that ultrasound elastography techniques are difficult to be applied, such as imaging of the brain, MR ARF imaging is expected to play an important role in tissue characterization and treatment monitoring.

ACKNOWLEDGMENTS

The authors thank Peter Siegler for advice on the MR sequence and Shawna Rideout-Gros for helping with the animal studies and acknowledge the funding support from NIH Grant No. R33 CA102884, CRC program, and Terry Fox Foundation. Contract grant sponsor is NIH Grant No. R21/R33 CA102884-01.

[a]Electronic mail: huangyx@sten.sunnybrook.utoronto.ca; Telephone: (416) 480-6100 ext. 89418; Fax: (416) 480-4696.
[b]Electronic mail: curiell@tbh.net; Telephone: (416) 480-6100 ext. 89415; Fax: (416) 480-4696.
[c]Electronic mail: akukic@sri.utoronto.ca; Telephone: (416) 480-6100 ext. 89414; Fax: (416) 480-4696.
[d]Electronic mail: don.plewes@sw.ca; Telephone: (416) 480-5709; Fax: (416) 480-5714.
[e]Electronic mail: rajiv.chopra@sri.utoronto.ca; Telephone: (416) 480-6100 ext. 6084; Fax: (416) 480-4696.
[f]Author to whom correspondence should be addressed. Electronic mail: khynynen@sri.utoronto.ca; Telephone: (416) 480-5717; Fax: (416) 480-5714.

[1]R. M. Lerner, S. R. Huang, and K. J. Parker, "'Sonoelasticity' images derived from ultrasound signals in mechanically vibrated tissues," Ultrasound Med. Biol. **16**, 231–239 (1990).
[2]J. Ophir, I. Cespedes, H. Ponnekanti, Y. Yazdi, and X. Li, "Elastography: A quantitative method for imaging the elasticity of biological tissues," Ultrason. Imaging **13**, 111–134 (1991).
[3]I. Cespedes, J. Ophir, H. Ponnekanti, and N. Maklad, "Elastography: Elasticity imaging using ultrasound with application to muscle and breast in vivo," Ultrason. Imaging **15**, 73–88 (1993).
[4]M. O'Donnell, A. R. Skovoroda, B. M. Shapo, and S. Y. Emelianov, "Internal displacement and strain imaging using ultrasonic speckle tracking," IEEE Trans. Ultrason. Ferroelectr. Freq. Control **41**, 314–325 (1994).
[5]R. Muthupillai, D. J. Lomas, P. J. Rossman, J. F. Greenleaf, A. Manduca, and R. L. Ehman, "Magnetic resonance elastography by direct visualization of propagating acoustic strain waves," Science **269**, 1854–1857 (1995).
[6]D. B. Plewes, I. Betty, S. N. Urchukm, and I. Soutar, "Visualizing tissue compliance with MR imaging," J. Magn. Reson. Imaging **5**, 733–738 (1995).
[7]A. Manduca, R. Muthupillai, P. J. Rossman, J. F. Greenleaf, and R. L. Ehman, "Image processing for magnetic resonance elastography," Proc. SPIE **2710**, 616–623 (1996).
[8]A. P. Sarvazyan, O. V. Rudenko, S. D. Swanson, J. B. Fowlkes, and S. Y. Emelianov, "Shear wave elasticity imaging: A new ultrasonic technology of medical diagnostics," Ultrasound Med. Biol. **24**, 1419–1435 (1998).
[9]T. Wu, J. P. Felmlee, J. F. Greenleaf, S. J. Riederer, and R. L. Ehman, "MR imaging of shear waves generated by focused ultrasound," Magn. Reson. Med. **43**, 111–115 (2000).
[10]K. R. Nightingale, M. L. Palmeri, R. W. Nightingale, and G. E. Trahey, "On the feasibility of remote palpation using acoustic radiation force," J. Acoust. Soc. Am. **110**, 625–634 (2001).

[11]L. Yuan, K. J. Glaser, O. Rouviere, K. R. Gorny, S. Chen, A. Manduca, R. L. Ehman, and J. P. Felmlee, "Preliminary assessment of one-dimensional MR elastography for use in monitoring focused ultrasound therapy," Phys. Med. Biol. **52**, 5909–5919 (2007).
[12]N. McDannold and S. E. Maier, "Magnetic resonance acoustic radiation force imaging," Med. Phys. **35**, 3748–3758 (2008).
[13]R. Souchon, R. Salomir, O. Beuf, L. Milot, D. Grenier, D. Lyonnet, J. Chapelon, and O. Rouviere, "Transient MR elastography (t-MRE) using ultrasound radiation force: Theory, safety, and initial experiments in vitro," Magn. Reson. Med. **60**, 871–881 (2008).
[14]E. E. Konofagou and K. Hynynen, "Localized harmonic motion imaging: Theory, simulations and experiments," Ultrasound Med. Biol. **29**, 1405–1413 (2003).
[15]L. Curiel, R. Chopra, and K. Hynynen, "In vivo monitoring of focused ultrasound surgery using local harmonic motion," Ultrasound Med. Biol. **35**, 65–78 (2009).
[16]C. Maleke, M. Pernot, and E. E. Konofagou, "Single-element focused ultrasound transducer method for harmonic motion imaging," Ultrason. Imaging **24**, 2001–2010 (2006).
[17]Y. Wang and D. B. Plewes, "An MRI calorimetry technique to measure tissue ultrasound absorption," Magn. Reson. Med. **42**, 158–166 (1999).
[18]N. J. McDannold, R. L. King, F. A. Jolesz, and K. H. Hynynen, "Usefulness of MR imaging-derived thermometry and dosimetry in determining the threshold for tissue damage induced by thermal surgery in rabbits," Radiology **216**, 517–523 (2000).